The influence of organic bases and substituted groups upon coordination structures affording two mononuclear Dy (III) single-molecule magnets (SMMs) and a novel Dy (III)-K (I) compound with unusual coordinated fluorine atoms

Nan Shen,[a#] Jing Liang,[d#] Xiaoni Qu,[e] Liu Sha,[a] Lin Zhu,[a] Sheng Zhang,[*a] Ling Chen,[*d] Jiangwei Zhang,[c] Dengwei Hu,[a] Bing Yin[*b]

AUTHOR ADDRESS

a. *Faculty of Chemistry and Chemical Engineering, Engineering Research Center of Advanced Ferroelectric Functional Materials, Key Laboratory of Phytochemistry of Shaanxi Province, Baoji University of Arts and Sciences, 1 Hi-Tech Avenue, Baoji, Shaanxi, 721013, China*
b. *Key Laboratory of Synthetic and Natural Functional Molecule Chemistry of Ministry of Education, College of Chemistry and Materials Science, Northwest University, Xi'an, Shaanxi 710069, China*
c. *State Key Laboratory of Catalysis, Dalian Institute of Chemical Physics, Chinese Academy of Sciences (CAS) Dalian 116023, P.R.China*
d. *Shannxi Provincial Cancer Hospital, Xi' an 710069, China*
e. *College of Environment and Chemistry Engineering, Xi'an Polytechnic University, Xi'an 710048, P. R China.*

[#]These authors contributed equally to this work.

Corresponding Authors

***E-mail: zhangsheng19890501@163.com. (S. Zhang)**

***E-mail: rayinyin@nwu.edu.cn. (B. Yin)**

***E-mail: 27376231@qq.com (C. Chen)**

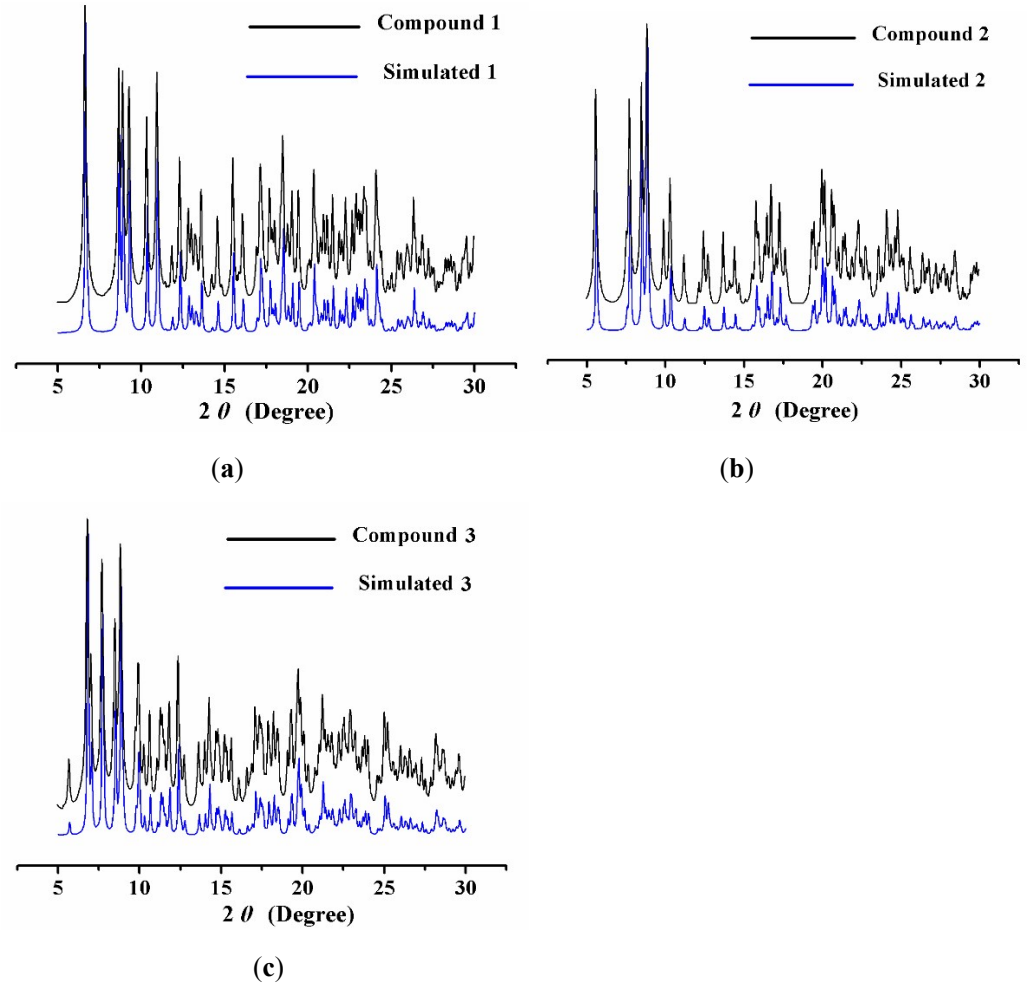

Fig. S1 XRPD curves of **1-3** (**a** to **c**).

Table S1 Bond lengths and bond angles for **1**.

1			
Dy(1)-O(6)	2.313(9)	O(6)-Dy(1)-O(3)	74.2(3)
Dy(1)-O(4)	2.319(10)	O(4)-Dy(1)-O(3)	72.0(3)
Dy(1)-O(2)	2.328(9)	O(2)-Dy(1)-O(3)	73.9(3)
Dy(1)-O(5)	2.329(9)	O(5)-Dy(1)-O(3)	133.4(3)
Dy(1)-O(1)	2.331(8)	O(1)-Dy(1)-O(3)	126.3(3)
Dy(1)-O(3)	2.346(9)	O(6)-Dy(1)-N(1)	100.7(3)
Dy(1)-N(1)	2.519(10)	O(4)-Dy(1)-N(1)	145.1(3)
Dy(1)-N(2)	2.530(10)	O(2)-Dy(1)-N(1)	87.8(3)
O(6)-Dy(1)-O(4)	87.2(3)	O(5)-Dy(1)-N(1)	75.3(3)
O(6)-Dy(1)-O(2)	136.7(3)	O(1)-Dy(1)-N(1)	75.0(3)
O(4)-Dy(1)-O(2)	109.6(3)	O(3)-Dy(1)-N(1)	142.8(3)
O(6)-Dy(1)-O(5)	72.1(3)	O(6)-Dy(1)-N(2)	75.8(3)
O(4)-Dy(1)-O(5)	75.0(3)	O(4)-Dy(1)-N(2)	150.6(3)
O(2)-Dy(1)-O(5)	149.8(3)	O(2)-Dy(1)-N(2)	70.7(3)
O(6)-Dy(1)-O(1)	151.3(3)	O(5)-Dy(1)-N(2)	120.2(3)

O(4)-Dy(1)-O(1)	81.9(3)	O(1)-Dy(1)-N(2)	123.7(3)
O(2)-Dy(1)-O(1)	72.0(3)	O(3)-Dy(1)-N(2)	80.3(3)
O(5)-Dy(1)-O(1)	79.4(3)	N(1)-Dy(1)-N(2)	63.0(3)

Table S2 Bond lengths and bond angles for **2**.

2			
Dy1-K1	3.9419(7)	F4-K1-F4^{1}	180
Dy1-O1	2.347(6)	F10-K1-F2	118.9(2)
Dy1-O2	2.350(7)	F10-K1-F2^{1}	61.1(2)
Dy1-O3	2.388(7)	F10^{1}-K1-F2	61.1(2)
Dy1-O4	2.336(7)	F10^{1}-K1-F2^{1}	118.9(2)
Dy1-O5	2.370(8)	F10-K1-F4^{1}	59.2(2)
Dy1-O6	2.315(8)	F10^{1}-K1-F4^{1}	120.8(2)
Dy1-O7	2.379(7)	F10-K1-F4	120.8(2)
Dy1-O8	2.318(7)	F10^{1}-K1-F4	59.2(2)
K1-F2^{1}	2.983(7)	F10^{1}-K1-F10	180
K1-F2	2.983(7)	O1^{1}-K1-F2^{1}	56.11(18)
K1-F4^{1}	3.023(8)	O1^{1}-K1-F2	123.89(18)
K1-F4	3.023(8)	O1-K1-F2	56.11(18)
K1-F10	2.939(7)	O1-K1-F2^{1}	123.89(18)
K1-F10^{1}	2.939(7)	O1^{1}-K1-F4	74.4(2)
K1-O1^{1}	2.777(7)	O1-K1-F4^{1}	74.4(2)
K1-O1	2.777(7)	O1^{1}-K1-F4^{1}	105.6(2)
K1-O3^{1}	2.936(7)	O1-K1-F4	105.6(2)
K1-O3	2.936(7)	O1-K1-F10	106.6(2)
K1-O7^{1}	2.831(7)	O1^{1}-K1-F10^{1}	106.6(2)
K1-O7	2.831(7)	O1^{1}-K1-F10	73.4(2)
O1-Dy1-K1	43.88(17)	O1-K1-F10^{1}	73.4(2)
O1-Dy1-O2	72.8(2)	O1^{1}-K1-O1	180
O1-Dy1-O3	76.6(3)	O1^{1}-K1-O3	118.2(2)
O1-Dy1-O5	113.4(3)	O1-K1-O3	61.8(2)
O1-Dy1-O7	79.4(2)	O1^{1}-K1-O3^{1}	61.8(2)
O2-Dy1-K1	99.85(17)	O1-K1-O3^{1}	118.3(2)
O2-Dy1-O3	80.2(3)	O1^{1}-K1-O7	114.8(2)
O2-Dy1-O5	73.6(3)	O1-K1-O7^{1}	114.8(2)
O2-Dy1-O7	145.1(2)	O1-K1-O7	65.2(2)
O3-Dy1-K1	47.90(16)	O1^{1}-K1-O7^{1}	65.2(2)
O4-Dy1-K1	119.02(18)	O31-K1-F2^{1}	109.4(2)
O4-Dy1-O1	139.2(3)	O3-K1-F2	109.44(19)
O4-Dy1-O2	76.6(2)	O3-K1-F2^{1}	70.56(19)
O4-Dy1-O3	72.1(2)	O3^{1}-K1-F2	70.56(19)
O4-Dy1-O5	82.2(3)	O3^{1}-K1-F4	128.22(19)

O4-Dy1-O7	114.5(3)	O3-K1-F4	51.77(19)
O5-Dy1-K1	156.4(2)	O3-K1-F4^{1}	128.23(19)
O5-Dy1-O3	146.8(3)	O3^{1}-K1-F4^{1}	51.77(19)
O5-Dy1-O7	138.5(3)	O3-K1-F10	107.41(19)
O6-Dy1-K1	90.82(19)	O3^{1}-K1-F10^{1}	107.41(19)
O6-Dy1-O1	73.1(3)	O3^{1}-K1-F10	72.59(19)
O6-Dy1-O2	115.8(3)	O3-K1-F10^{1}	72.59(19)
O6-Dy1-O3	138.6(3)	O3^{1}-K1-O3	180
O6-Dy1-O4	146.2(3)	O7^{1}-K1-F2^{1}	114.2(2)
O6-Dy1-O5	72.7(3)	O7^{1}-K1-F2	65.8(2)
O6-Dy1-O7	74.2(3)	O7-K1-F2^{1}	65.8(2)
O6-Dy1-O8	80.4(3)	O7-K1-F2	114.2(2)
O7-Dy1-K1	45.33(16)	O7^{1}-K1-F4	79.1(2)
O7-Dy1-O3	73.0(2)	O7^{1}-K1-F4^{1}	100.9(2)
O8-Dy1-K1	116.87(17)	O7-K1-F4^{1}	79.1(2)
O8-Dy1-O1	145.6(3)	O7-K1-F4	100.9(2)
O8-Dy1-O2	140.1(2)	O7^{1}-K1-F10	126.56(18)
O8-Dy1-O3	112.4(3)	O7^{1}-K1-F10^{1}	53.44(18)
O8-Dy1-O4	72.4(3)	O7-K1-F10^{1}	126.56(18)
O8-Dy1-O5	77.8(3)	O7-K1-F10	53.44(18)
O8-Dy1-O7	72.5(2)	O7-K1-O3^{1}	121.1(2)
F2-K1-F2^{1}	180	O7-K1-O3	58.9(2)
F2-K1-F4^{1}	59.7(2)	O7^{1}-K1-O3^{1}	58.9(2)
F2^{1}-K1-F4	59.7(2)	O7^{1}-K1-O3	121.1(2)
F2-K1-F4	120.3(2)	O7^{1}-K1-O7	180
F2^{1}-K1-F4^{1}	120.3(2)		

Table S3 Bond lengths and bond angles for **3**.

3			
Dy(1)-O(1)	2.296(7)	O(2)-Dy(1)-N(2)	71.0(3)
Dy(1)-O(3)	2.302(7)	O(5)-Dy(1)-N(2)	83.7(3)
Dy(1)-O(6)	2.308(8)	O(1)-Dy(1)-N(1)	74.9(3)
Dy(1)-O(4)	2.311(7)	O(3)-Dy(1)-N(1)	135.4(3)
Dy(1)-O(2)	2.318(7)	O(4)-Dy(1)-N(1)	149.4(3)
Dy(1)-O(5)	2.364(7)	O(6)-Dy(1)-N(1)	82.6(2)
Dy(1)-N(2)	2.554(8)	O(2)-Dy(1)-N(1)	114.4(3)
Dy(1)-N(1)	2.590(7)	O(5)-Dy(1)-N(1)	72.1(3)
Dy(2)-O(10)	2.301(8)	O(10)-Dy(2)-O(12)	82.0(3)
Dy(2)-O(12)	2.330(8)	O(10)-Dy(2)-O(11)	81.8(3)
Dy(2)-O(11)	2.318(9)	O(12)-Dy(2)-O(11)	71.9(3)
Dy(2)-O(9)	2.327(9)	O(10)-Dy(2)-O(9)	73.2(3)
Dy(2)-O(8)	2.320(7)	O(12)-Dy(2)-O(9)	143.1(3)
Dy(2)-O(7)	2.381(8)	O(11)-Dy(2)-O(9)	77.8(3)

Dy(2)-N(6)	2.543(9)	O(10)-Dy(2)-O(8)	74.3(3)
Dy(2)-N(5)	2.551(8)	O(12)-Dy(2)-O(8)	74.2(3)
O(1)-Dy(1)-O(3)	143.5(3)	O(11)-Dy(2)-O(8)	140.7(3)
O(1)-Dy(1)-O(6)	79.4(3)	O(9)-Dy(2)-O(8)	122.5(3)
O(3)-Dy(1)-O(6)	118.3(3)	O(10)-Dy(2)-O(7)	103.4(3)
O(1)-Dy(1)-O(4)	83.2(3)	O(12)-Dy(2)-O(7)	141.8(3)
O(3)-Dy(1)-O(4)	73.8(3)	O(11)-Dy(2)-O(7)	146.1(3)
O(4)-Dy(1)-O(6)	72.5(3)	O(9)-Dy(2)-O(7)	72.0(3)
O(1)-Dy(1)-O(2)	72.1(2)	O(8)-Dy(2)-O(7)	71.2(3)
O(3)-Dy(1)-O(2)	75.4(3)	O(10)-Dy(2)-N(6)	145.7(3)
O(4)-Dy(1)-O(2)	77.5(3)	O(12)-Dy(2)-N(6)	111.1(3)
O(6)-Dy(1)-O(2)	140.6(3)	O(11)-Dy(2)-N(6)	73.2(3)
O(1)-Dy(1)-O(5)	138.8(2)	O(9)-Dy(2)-N(6)	78.8(3)
O(3)-Dy(1)-O(5)	77.5(3)	O(8)-Dy(2)-N(6)	139.0(3)
O(4)-Dy(1)-O(5)	115.1(3)	O(7)-Dy(2)-N(6)	85.9(3)
O(6)-Dy(1)-O(5)	72.6(3)	O(10)-Dy(2)-N(5)	149.3(3)
O(2)-Dy(1)-O(5)	145.2(3)	O(12)-Dy(2)-N(5)	77.2(3)
O(1)-Dy(1)-N(2)	103.1(3)	O(11)-Dy(2)-N(5)	112.1(3)
O(3)-Dy(1)-N(2)	81.4(3)	O(9)-Dy(2)-N(5)	135.2(3)
O(4)-Dy(1)-N(2)	143.9(3)	O(8)-Dy(2)-N(5)	78.4(3)
O(6)-Dy(1)-N(2)	143.5(3)	O(7)-Dy(2)-N(5)	80.6(3)

Table S4 Dy^{III} ion geometry analysis by SHAPE 2.1 software.

Configuration	ABOXIY, **1**	ABOXIY, **2**	ABOXIY, **3Dy1**	ABOXIY, **3Dy2**
Octagon(D8h)	30.583	29.707	30.961	31.484
Heptagonal pyramid(C7v)	23.031	23.736	21.180	23.014
Hexagonal bipyramid(D6h)	13.824	15.949	15.004	16.236
Cube(Oh)	7.452	8.592	8.965	9.768
Square antiprism (D_{4d})	1.552	0.247	0.740	0.910
Triangular dodecahedron (D_{2d})	0.702	2.269	1.811	1.730
Johnson gyrobifastigium J26 (D_{2d})	15.424	16.286	15.406	15.113
Johnson elongated triangular bipyramid J14 (D_{3h})	28.336	29.181	27.911	28.116
Biaugmented trigonal prism J50 (C_{2v})	2.832	2.926	2.482	2.455
Biaugmented trigonal prism (C_{2v})	2.241	2.341	2.043	1.605
Snub siphenoid J84 (D_{2d})	3.798	5.390	4.829	4.606
Triakis tetrahedron(Td)	8.204	9.388	9.792	10.582

Elongated trigonal bipyramid(D3h)	23.012	24.142	24.335	23.994

Table S5 K (I) ion geometry analysis by SHAPE 2.1 software.

Configuration	ABOXIY, 2**K**
Dodecagon (D_{12h})	34.311
Hendecagonal pyramid(C_{11v})	28.356
Decagonal bipyramid(D_{10h})	15.497
Hexagonal prism(D_{6h})	8.298
Hexagonal antiprism(D_{6d})	14.369
Truncated tetrahedron (T_d)	13.237
Cuboctahedron (O_h)	2.979
Anticuboctahedron J27(D_{3h})	4.717
Icosahedron (I_h)	2.069
Johnson square cupola J4(C_{4v})	20.489
Johnson elongated pentagonal bipyramid J16(D_{6h})	7.932
Biaugmented pentagonal prism J53(C_{2v})	13.200
Sphenomegacorona J88(C_s)	17.658

--1----------

S H A P E v2.1 Continuous Shape Measures calculation

(c) 2013 Electronic Structure Group, Universitat de Barcelona

Contact: llunell@ub.edu

Dy structures

OP-8	1 D8h	Octagon
HPY-8	2 C7v	Heptagonal pyramid
HBPY-8	3 D6h	Hexagonal bipyramid
CU-8	4 Oh	Cube
SAPR-8	5 D4d	Square antiprism
TDD-8	6 D2d	Triangular dodecahedron
JGBF-8	7 D2d	Johnson gyrobifastigium J26
JETBPY-8	8 D3h	Johnson elongated triangular bipyramid J14
JBTPR-8	9 C2v	Biaugmented trigonal prism J50
BTPR-8	10 C2v	Biaugmented trigonal prism
JSD-8	11 D2d	Snub diphenoid J84
TT-8	12 Td	Triakis tetrahedron
ETBPY-8	13 D3h	Elongated trigonal bipyramid

Structure [ML8] OP-8 HPY-8 HBPY-8 CU-8 SAPR-8 TDD-8 JGBF-8 JETBPY-8 JBTPR-8 BTPR-8 JSD-8 TT-8 ETBPY-8
ABOXIY , 30.583, 23.031, 13.824, 7.452, 1.552, 0.702, 15.424, 28.336, 2.832, 2.241, 3.798, 8.204, 23.012

2

S H A P E v2.1 Continuous Shape Measures calculation
(c) 2013 Electronic Structure Group, Universitat de Barcelona
Contact: llunell@ub.edu

Dy structures

OP-8	1 D8h	Octagon
HPY-8	2 C7v	Heptagonal pyramid
HBPY-8	3 D6h	Hexagonal bipyramid
CU-8	4 Oh	Cube
SAPR-8	5 D4d	Square antiprism
TDD-8	6 D2d	Triangular dodecahedron
JGBF-8	7 D2d	Johnson gyrobifastigium J26
JETBPY-8	8 D3h	Johnson elongated triangular bipyramid J14
JBTPR-8	9 C2v	Biaugmented trigonal prism J50
BTPR-8	10 C2v	Biaugmented trigonal prism
JSD-8	11 D2d	Snub diphenoid J84
TT-8	12 Td	Triakis tetrahedron
ETBPY-8	13 D3h	Elongated trigonal bipyramid

Structure [ML8] OP-8 HPY-8 HBPY-8 CU-8 SAPR-8 TDD-8 JGBF-8 JETBPY-8 JBTPR-8 BTPR-8 JSD-8 TT-8 ETBPY-8
ABOXIY , 29.707, 23.736, 15.949, 8.592, 0.274, 2.269, 16.286, 29.181, 2.926, 2.341, 5.390, 9.388, 24.142

S H A P E v2.1 Continuous Shape Measures calculation
(c) 2013 Electronic Structure Group, Universitat de Barcelona
Contact: llunell@ub.edu

2

S H A P E v2.1 Continuous Shape Measures calculation

(c) 2013 Electronic Structure Group, Universitat de Barcelona
Contact: llunell@ub.edu

K structures

DP-12	1	D12h	Dodecagon
HPY-12	2	C11v	Hendecagonal pyramid
DBPY-12	3	D10h	Decagonal bipyramid
HPR-12	4	D6h	Hexagonal prism
HAPR-12	5	D6d	Hexagonal antiprism
TT-12	6	Td	Truncated tetrahedron
COC-12	7	Oh	Cuboctahedron
ACOC-12	8	D3h	Anticuboctahedron J27
IC-12	9	Ih	Icosahedron
JSC-12	10	C4v	Johnson square cupola J4
JEPBPY-12	11	D6h	Johnson elongated pentagonal bipyramid J16
JBAPPR-12	12	C2v	Biaugmented pentagonal prism J53
JSPMC-12	13	Cs	Sphenomegacorona J88

Structure [ML12]	DP-12	HPY-12	DBPY-12	HPR-12	HAPR-12	TT-12	COC-12	ACOC-12	IC-12	JSC-12	JEPBPY-12	JBAPPR-12	JSPMC-12
ABOXIY	34.311,	28.356,	15.497,	8.298,	14.369,	13.237,	2.979,	4.717,	2.069,	20.489,	7.932,	13.200,	17.658

S H A P E v2.1 Continuous Shape Measures calculation
(c) 2013 Electronic Structure Group, Universitat de Barcelona
Contact: llunell@ub.edu

3DY1
Dy structures

OP-8	1	D8h	Octagon
HPY-8	2	C7v	Heptagonal pyramid
HBPY-8	3	D6h	Hexagonal bipyramid
CU-8	4	Oh	Cube
SAPR-8	5	D4d	Square antiprism
TDD-8	6	D2d	Triangular dodecahedron
JGBF-8	7	D2d	Johnson gyrobifastigium J26
JETBPY-8	8	D3h	Johnson elongated triangular bipyramid J14
JBTPR-8	9	C2v	Biaugmented trigonal prism J50
BTPR-8	10	C2v	Biaugmented trigonal prism

JSD-8 11 D2d Snub diphenoid J84
TT-8 12 Td Triakis tetrahedron
ETBPY-8 13 D3h Elongated trigonal bipyramid

Structure [ML8] OP-8 HPY-8 HBPY-8 CU-8 SAPR-8 TDD-8 JGBF-8 JETBPY-8 JBTPR-8 BTPR-8 JSD-8 TT-8 ETBPY-8
ABOXIY , 30.961, 21.180, 15.004, 8.965, 0.740, 1.811, 15.406, 27.911, 2.482, 2.043, 4.829, 9.792, 24.335

S H A P E v2.1 Continuous Shape Measures calculation
(c) 2013 Electronic Structure Group, Universitat de Barcelona
Contact: llunell@ub.edu

3DY2
Dy structures

OP-8 1 D8h Octagon
HPY-8 2 C7v Heptagonal pyramid
HBPY-8 3 D6h Hexagonal bipyramid
CU-8 4 Oh Cube
SAPR-8 5 D4d Square antiprism
TDD-8 6 D2d Triangular dodecahedron
JGBF-8 7 D2d Johnson gyrobifastigium J26
JETBPY-8 8 D3h Johnson elongated triangular bipyramid J14
JBTPR-8 9 C2v Biaugmented trigonal prism J50
BTPR-8 10 C2v Biaugmented trigonal prism
JSD-8 11 D2d Snub diphenoid J84
TT-8 12 Td Triakis tetrahedron
ETBPY-8 13 D3h Elongated trigonal bipyramid

Structure [ML8] OP-8 HPY-8 HBPY-8 CU-8 SAPR-8 TDD-8 JGBF-8 JETBPY-8 JBTPR-8 BTPR-8 JSD-8 TT-8 ETBPY-8
ABOXIY , 31.484, 23.014, 16.236, 9.768, 0.910, 1.730, 15.113, 28.116, 2.455, 1.605, 4.606, 10.582, 23.994

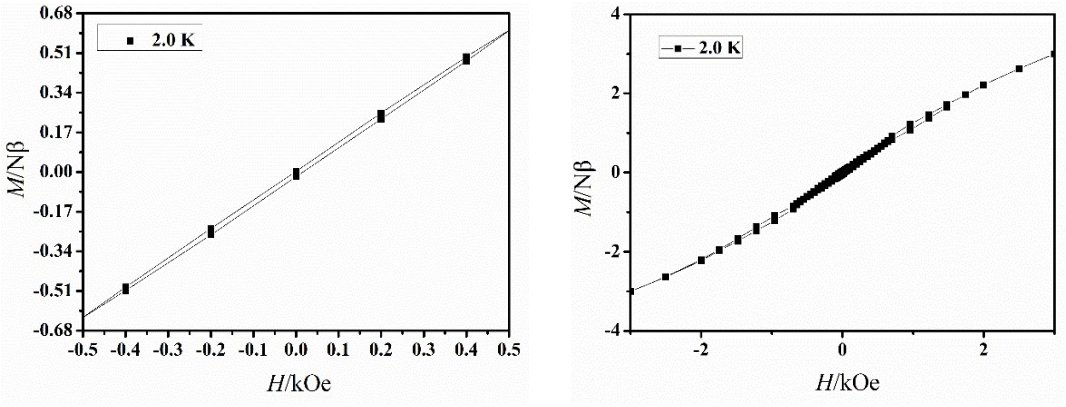

(a) **(b)**

Fig. S1 Magnetic hysteresis loops for compounds **1** (a) and **3** (b), respectively.

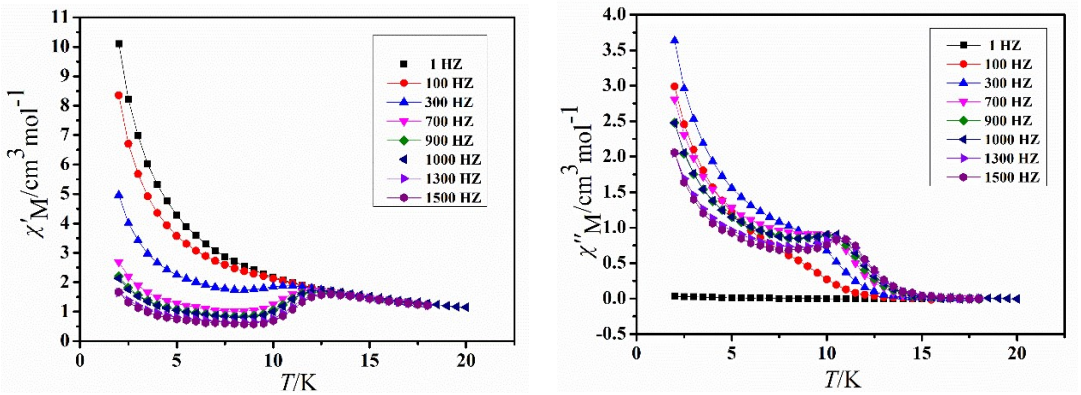

(a) **(b)**

Fig. S2 Temperature dependence of the in-phase (χ', a) and out-of-phase (χ'', b) ac susceptibility signals under 0 Oe dc field for **1**.

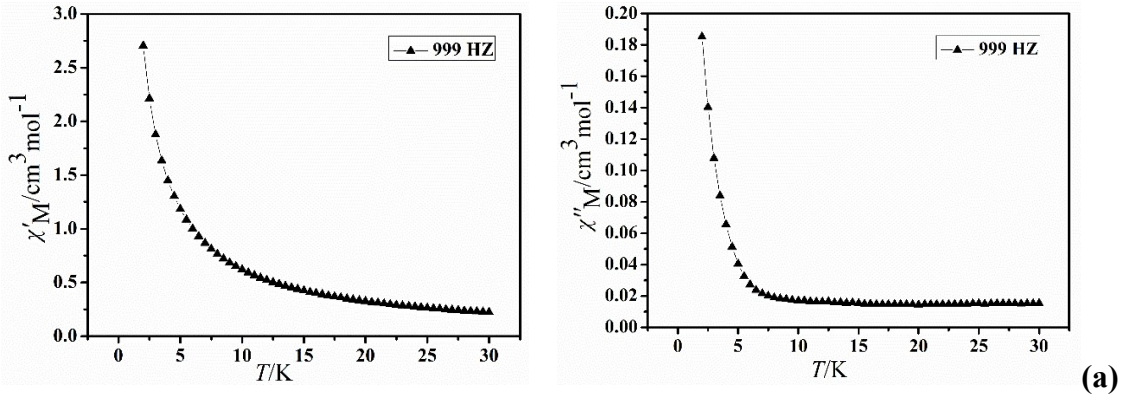

(b) **(a)**

Fig. S3 Temperature dependence of the in-phase (χ', a) and out-of-phase (χ'', b) ac susceptibility signals under 0 Oe dc field for **2**.

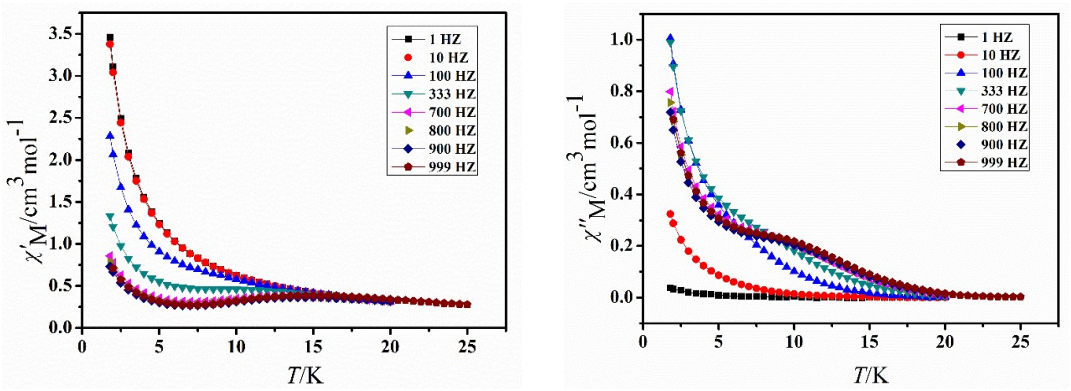

(a) **(b)**

Fig. S4 Temperature dependence of the in-phase (χ', a) and out-of-phase (χ'', b) ac susceptibility signals under 0 Oe dc field for **3**.

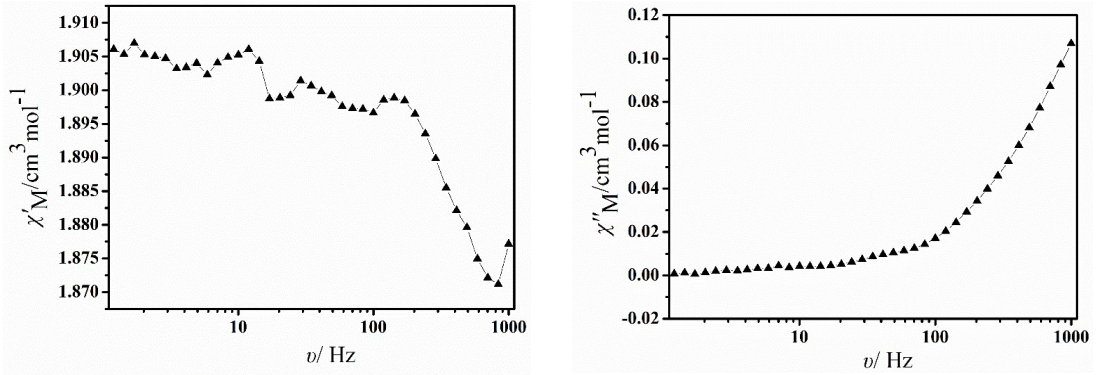

(a) **(b)**

Fig. S5 Plots of the frequency-dependent in-phase (a) and out-of-phase (b) ac susceptibility at indicated temperatures for **2**.

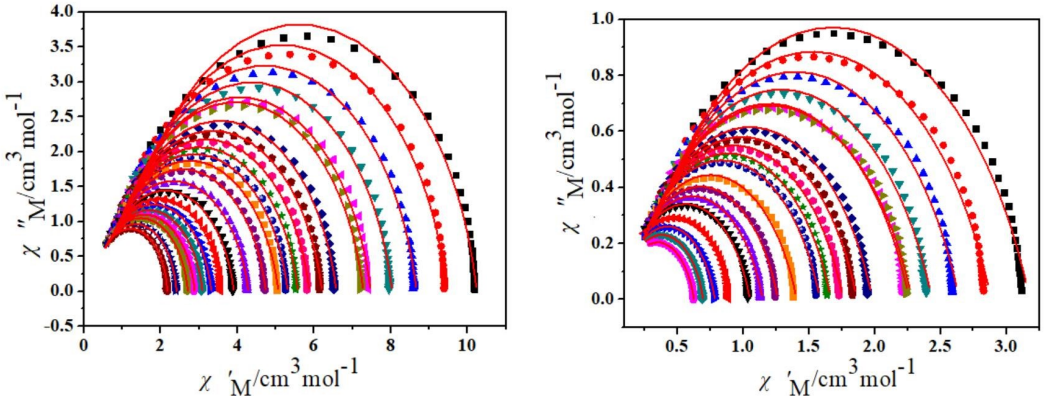

(a) **(b)**

Fig. S6 Cole–Cole diagrams with red solid lines as Debye fits for **1** (a) and **3** (b), respectively.

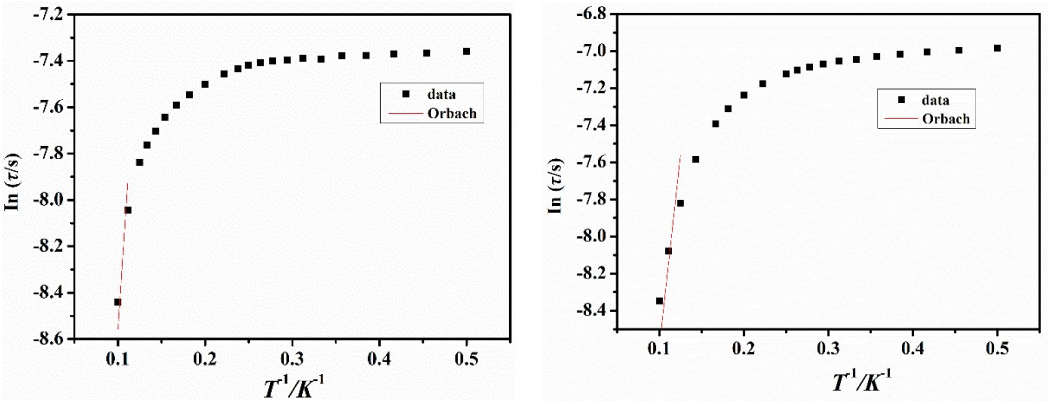

Fig. S7 Fitting of frequency dependence of relaxation time under 0 Oe dc field for **1** (a) and **3** (d).

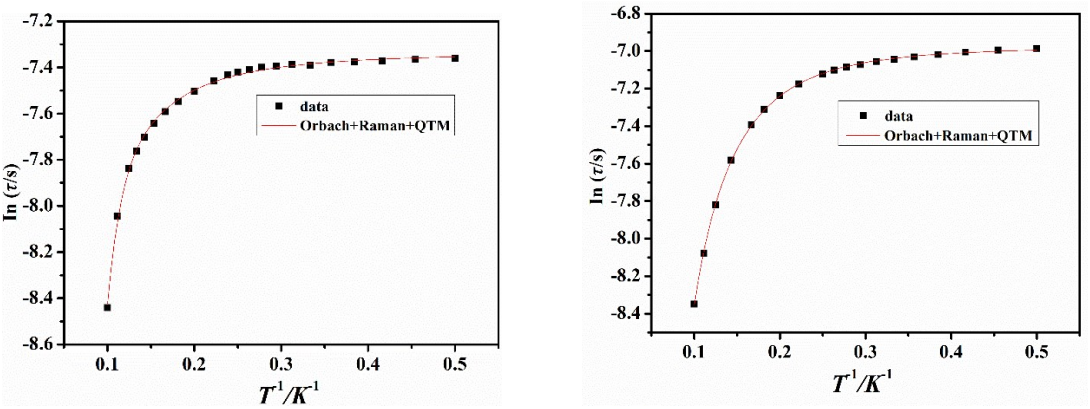

Fig. S8 Fitting of frequency dependence of relaxation time under 0 Oe dc field for **1** (a) and **3** (b).

4. Relaxation fitting parameters of 1 and 3

The magnetic susceptibility data of **1** and **3** under a zero dc field were described by the modified Debye functions:

$$\chi'(\omega) = \chi_S + (\chi_T - \chi_S)\frac{1+(\omega\tau)^{1-\alpha}\sin(\frac{\pi}{2}\alpha)}{1+2(\omega\tau)^{1-\alpha}\sin(\frac{\pi}{2}\alpha)+(\omega\tau)^{(2-2\alpha)}}$$

$$\chi''(\omega) = (\chi_T - \chi_S)\frac{(\omega\tau)^{1-\alpha}\cos(\frac{\pi}{2}\alpha)}{1+2(\omega\tau)^{1-\alpha}\sin(\frac{\pi}{2}\alpha)+(\omega\tau)^{(2-2\alpha)}}$$

$$\chi''_{\omega=\tau^{-1}} = (\chi_T - \chi_S)\frac{\cos(\frac{\pi}{2}\alpha)}{2+2\sin(\frac{\pi}{2}\alpha)} = \frac{1}{2}(\chi_T - \chi_S)\tan\frac{\pi}{4}(1-\alpha)$$

Table S6 Relaxation fitting parameters from Least-Squares Fitting of $\chi(\omega)$ data for **1** under a zero applied dc field.

T	$\Delta\chi_1$ (cm^3mol^{-1})	$\Delta\chi_2$ (cm^3mol^{-1})	τ(s)	α
2	0.983532E+00	0.102372E+02	0.636214E-03	0.120707E+00
2.2	0.877062E+00	0.946374E+01	0.632538E-03	0.124239E+00
2.4	0.770546E+00	0.866756E+01	0.629372E-03	0.126738E+00
2.6	0.698238E+00	0.803123E+01	0.626111E-03	0.128596E+00
2.8	0.641316E+00	0.747214E+01	0.625104E-03	0.129681E+00
3	0.624238E+00	0.728084E+01	0.616214E-03	0.129649E+00
3.2	0.550759E+00	0.657650E+01	0.618803E-03	0.132735E+00
3.4	0.512913E+00	0.620566E+01	0.614080E-03	0.134195E+00
3.6	0.493857E+00	0.587573E+01	0.611164E-03	0.133591E+00
3.8	0.470212E+00	0.558001E+01	0.605921E-03	0.134295E+00
4	0.450917E+00	0.531156E+01	0.598924E-03	0.133974E+00
4.2	0.432325E+00	0.506660E+01	0.591299E-03	0.134823E+00
4.5	0.405041E+00	0.474123E+01	0.577360E-03	0.135353E+00
5	0.369947E+00	0.428356E+01	0.551649E-03	0.134736E+00
5.5	0.350855E+00	0.390603E+01	0.527635E-03	0.130152E+00
6	0.338212E+00	0.358603E+01	0.504476E-03	0.125414E+00
6.5	0.311197E+00	0.331829E+01	0.479174E-03	0.120318E+00
7	0.296681E+00	0.308618E+01	0.451865E-03	0.114586E+00
7.5	0.280323E+00	0.288362E+01	0.425154E-03	0.105898E+00
8	0.263316E+00	0.270553E+01	0.394531E-03	0.961469E-01
9	0.248838E+00	0.240956E+01	0.320753E-03	0.715124E-01
10	0.246896E+00	0.216867E+01	0.215905E-03	0.446681E-01

Table S7 Relaxation fitting parameters from Least-Squares Fitting of $\chi(\omega)$ data for **3** under a zero applied dc field.

T	$\Delta\chi_1$ (cm^3mol^{-1})	$\Delta\chi_2$ (cm^3mol^{-1})	τ(s)	α
2	0.185550E+00	0.317884E+01	0.925102E-03	0.266784E+00
2.2	0.170850E+00	0.288622E+01	0.916392E-03	0.264696E+00
2.4	0.158753E+00	0.264416E+01	0.907133E-03	0.262524E+00
2.6	0.145156E+00	0.243583E+01	0.895439E-03	0.261895E+00
2.8	0.138553E+00	0.226293E+01	0.885056E-03	0.258568E+00
3	0.136412E+00	0.228612E+01	0.8719226E-03	0.271652E+00

3.2	0.123162E+00	0.198348E+01	0.862860E-03	0.255475E+00
3.4	0.116027E+00	0.186665E+01	0.849252E-03	0.253949E+00
3.6	0.111270E+00	0.176254E+01	0.836905E-03	0.251964E+00
3.8	0.106701E+00	0.166932E+01	0.822410E-03	0.249706E+00
4	0.102304E+00	0.158522E+01	0.807290E-03	0.247897E+00
4.5	0.930493E-01	0.140774E+01	0.765119E-03	0.242585E+00
5	0.864061E-01	0.126604E+01	0.719709E-03	0.236547E+00
5.5	0.810821E-01	0.114932E+01	0.668790E-03	0.229794E+00
6	0.768344E-01	0.105254E+01	0.615543E-03	0.223005E+00
7	0.734337E-01	0.900058E+00	0.509261E-03	0.208746E+00
8	0.688963E-01	0.786364E+00	0.401615E-03	0.199448E+00
9	0.716034E-01	0.697934E+00	0.310514E-03	0.191284E+00
10	0.777849E-01	0.627784E+00	0.237063E-03	0.186805E+00

Theoretical methods and computational details

This section is supposed to be included in ESI.

Multiconfigurational *ab initio* calculations, including spin-orbit coupling (SOC), were performed on the experimental structures of the complexes here to explore their SMM propertiesy. This type of calculation includes two steps: [1] 1) a set of spin eigenstates, are obtained by the state-averaged (SA) CASSCF method; [2] 2) the low-lying SOC states, i.e., Kramers doublets (KD) herein, are obtained by state interaction which is the diagonalization of the SOC matrix in the space spanned by the spin eigenstates from the first step. In the CASSCF step, the active space consisted of 9 electrons in 7 orbitals and all the spin eigenstates of 21 sextets were included. Due to the hardware limitation, other highly excited quartets and doublets were not considered. The step of state interaction were performed by the RASSI-SO module [3] with the SOC integrals from the AMFI method. [4] The ANO-RCC basis sets, [5–7] including VTZP for Dy, VDZ for C and H as well as VDZP for other atoms, were used. All the calculations were carried out with the MOLCAS@UU, a version of MOLCAS 8.0[10,11] which is freely distributed for academic users. The SINGLE ANISO module [8,9], developed by Chibotaru and et al, was used to obtain the g-tensors, transition magnetic moments ameters characterizing the magnetic anisotropy.

References

[1] Javier Luzón and Roberta Sessoli. Lanthanides in molecular magnetism: so fascinating, so challenging. *Dalton Trans*, 41:13556–13567, 2012.

[2] Björn O. Roos, Peter R. Taylor, and Per. E. M. Siegbahn. A COMPLETE ACTIVE SPACE SCF METHOD (CASSCF) USING A DENSITY MATRIX FORMULATED SUPER-CI APPROACH. *Chem Phys*, 48:157–173, 1980.

[3] Per-åke Malmqvist, Björn O. Roos, and Bernd Schimmelpfennig. The restricted active space (RAS) state interaction approach with spin-orbit coupling. *Chem Phys Lett*, 357:230–240, 2002.

[4] Bernd A Hess, ChristelM Marian, UlfWahlgren, and Odd Gropen. A mean-field spin-orbit method applicable to correlated wavefunctions. *Chem Phys Lett*, 251:365–371, 1996.

[5] Björn O. Roos, Roland Lindh, Per-åke Malmqvist, Valera Veryazov, and Per-Olof Widmark. Main Group Atoms and
Dimers Studied with a New Relativistic ANO Basis Set. *J Phys Chem A*, 108(15):2851–2858, 2004.

[6] Björn O. Roos, Roland Lindh, Per-åke Malmqvist, Valera Veryazov, and Per-Olof Widmark. New Relativistic ANO Basis Sets for Transition Metal Atoms. *J Phys Chem A*, 109(29):6575–6579, 2005.

[7] Björn O. Roos, Roland Lindh, Per-åke Malmqvist, Valera Veryazov, Per-Olof Widmark, and Antonio Carlos Borin. New Relativistic Atomic Natural Orbital Basis Sets for Lanthanide Atoms with Applications to the Ce Diatom and LuF_3. *J Phys Chem A*, 112(45):11431–11435, 2008.

[8] Liviu F Chibotaru and Liviu Ungur. Ab initio calculation of anisotropic magnetic properties of complexes. I. Unique definition of pseudospin Hamiltonians and their derivation. *J Chem Phys*, 137:064112, 2012.

[9] Liviu F Chibotaru. *AB INITIO* METHODOLOGY FOR PSEUDOSPIN HAMILTONIANS OF ANISOTROPIC MAGNETIC COMPLEXES. *Adv Chem Phys*, 153:397–519, 2013.

[10] Francesco Aquilante, Luca De Vico, Nicolas Ferré, Giovanni Ghigo, Per-åke Malmqvist, Pavel Neogrády, Thomas Bondo Pedersen, Michal Pitoňák, Markus Reiher, Björn O. Roos, Luis Serrano-Andrés, Miroslav Urban, Valera Veryazov, and Roland Lindh. Molcas 7: The next generation. *J Comput Chem*, 31(1):224–247, 2010.

[11] Francesco Aquilante, Jochen Autschbach, Rebecca K. Carlson, Liviu F. Chibotaru, Mickael G. Delcey, Luca De Vico, Ignacio Fdez. Galván, Nicolas Ferré, Luis Manuel Frutos, Laura Gagliardi, Marco Garavelli, Angelo Giussani, Chad E. Hoyer, Giovanni Li Manni, Hans Lischka, Dongxia Ma, Per-åke Malmqvist, Thomas Müller, Artur Nenov, Massimo Olivucci, Thomas Bondo Pedersen, Daoling Peng, Felix Plasser, Ben Pritchard, Markus Reiher, Ivan Rivalta, Igor Schapiro, Javier Segarra-Martií, Michael Stenrup, Donald G. Truhlar, Liviu Ungur, Alessio Valentini, Steven Vancoillie, Valera Veryazov, Victor P. Vysotskiy, OliverWeingart, Felipe Zapata, and Roland Lindh. Molcas 8: New capabilities for multiconfigurational quantum chemical calculations across the periodic table. *J Comput Chem*, 37(5):506–541, 2016.